Contribution from the Institut für Anorganische und Analytische Chemie,
Johannes Gutenberg-Universität, D-6500 Mainz, West Germany

Mössbauer-Effect Study of the Thermally Induced Spin Transition in Tris(2-picolylamine)iron(II) Chloride. Dilution Effect in Mixed Crystals of $[Fe_xZn_{1-x}(2\text{-pic})_3]Cl_2 \cdot C_2H_5OH$ ($x = 0.15, 0.029, 0.0009$)

P. GÜTLICH,* R. LINK, and H. G. STEINHÄUSER[1]

Received January 19, 1978

The ^{57}Fe Mössbauer spectra of the polycrystalline mixed crystals $[Fe_xZn_{1-x}(2\text{-pic})_3]Cl_2 \cdot EtOH$ (2-pic = 2-picolylamine) have been measured at very low iron concentrations $x = 0.15$, 0.029, and 0.0009 and at temperatures between 5 and 300 K. The thermally induced high-spin ($^5T_2$) $\rightleftharpoons$ low-spin ($^1A_1$) transition, well established in the pure iron complex compound, is still observable at the lowest possible iron concentrations under study. With decreasing iron concentration, however, the transition temperature T_C is shifted to lower temperatures and the slope at T_C of the spin conversion function $\gamma_{HS}(T)$ becomes less steep, both facts being indicative of a weakening of the cooperative coupling between the electronic states and the phonon system. The results complement well those obtained in earlier studies on more concentrated mixed crystals, $0.2 \leq x \leq 1.0$. It has been found, however, that the empirical function $T_C(x)/K = 40x + 82$ deviates from linearity around $x \approx 0.15$ and falls off more rapidly than at higher iron concentrations, which apparently indicates that the presence of at least one next nearest iron complex molecule facilitates the "communication" of a primary spin transition throughout a cooperative domain via modulation of vibrational frequencies. A theoretical analysis of the temperature dependence of the quadrupole splitting of the iron(II) high-spin state, considering both cases of trigonal (C_{3v}) and rhombic (C_{2v}) distortion as well as spin–orbit coupling and covalency effects, has been made.

1. Introduction

The temperature-dependent low-spin ($^1A_1$) $\rightleftharpoons$ high-spin ($^5T_2$) transition, otherwise termed as magnetic crossover, in iron(II) complex compounds has been the subject of increasing interest in most recent years. Whereas the number of systems exhibiting this phenomenon is continuously growing, investigations aiming at a better understanding of the physical process and the mechanism of the spin transition are still relatively scarce.

On the basis of precise heat capacity measurements Sorai and Seki[2] have suggested that the spin transitions in $[Fe(phen)_2(NCS)_2]$ and $[Fe(phen)_2(NCSe)_2]$ (phen = 1,10-phenanthroline) are cooperative phenomena proceeding via significant coupling between the electronic state and the phonon system and that the spin conversion occurs simultaneously in a group of molecules forming a "cooperative domain".

In a more recent work performed by Sorai et al.[3] we proposed to examine more closely the suggested picture of cooperative spin transition in tris(2-picolylamine)iron(II) chloride, $[Fe(2\text{-pic})_3]Cl_2$ (2-pic = 2-picolylamine), for which the magnetic crossover has already been reported on briefly by Renovitch and Baker.[4] The solid solutions $[Fe_xZn_{1-x}(2\text{-pic})_3]Cl_2 \cdot C_2H_5OH$ have been found to be very suitable for a Mössbauer effect study of the dilution effect on the spin transition, because (i) iron(II) and zinc(II) form mixed crystals in the whole concentration range of interest and (ii) the variable-temperature ^{57}Fe Mössbauer spectra are composed of well-resolved quadrupole doublets originating from the high-spin and the low-spin species, respectively, whose gradually changing relative intensities may easily be followed as a function of temperature.[3a] In the concentration range $0.2 \leq x \leq 1.0$ one has indeed observed a pronounced dilution effect on the spin transition behavior in the sense that, at a given temperature, decreasing iron concentration favors the high-spin ($^5T_2$) state. Moreover, the transition temperature T_C has been found to vary linearly with the iron concentration in the range $0.2 \leq x \leq 1.0$ following the empirical relation $T_C(x)/K = 40x + 82$. These results, as well as those obtained from a similar study of the crystal solvent effect in the systems $[Fe(2\text{-pic})_3]Cl_2 \cdot Sol$ (Sol = CH_3OH, C_2H_5OH, H_2O, $2H_2O$)[3b] are in accordance with the suggested model of cooperative spin transition and have been extensively discussed, though qualitatively, in the framework of this model.[3a]

For several reasons it appeared to be highly desirable to pursue further the spin transition behavior in $[Fe_xZn_{1-x}(2\text{-pic})_3]Cl_2 \cdot C_2H_5OH$ to lowest possible iron concentrations. (i) The lowest iron concentration of $x = 0.2$ studied so far[3a] implies that each $[Fe(2\text{-pic})_3]^{2+}$ octahedron still has at least one complex iron ion as nearest neighbor playing a decisive role in communicating the primary spin change via spin–phonon coupling onto surrounding iron centers within the cooperative domain. The question therefore arises whether the linear $T_C(x)$ function of the range $0.2 \leq x \leq 1.0$[3b] experiences any noticeable deviation from linearity in the region of $x \leq 0.15$, where the $[Fe(2\text{-pic})_3]^{2+}$ cations are fully surrounded by $[Zn(2\text{-pic})_3]^{2+}$ neighbors. (ii) Particular interest is focused on the systems with extremely low iron concentrations to learn eventually whether, in contrast to magnetic spin ordering processes, a spin transition still takes place in individual iron centers far apart from each other and accommodated in a diamagnetic host matrix. (iii) Model calculations based on physically meaningful parameters should be performed and adjusted to the experimental data of $T_C(x)$ for a widest possible x dependence.

In this paper we communicate the experimental results of variable-temperature ^{57}Fe Mössbauer studies on $[Fe_xZn_{1-x}(2\text{-pic})_3]Cl_2 \cdot C_2H_5OH$ mixed crystals with $x = 0.15$, 0.029, and 0.0009. The quantitative theoretical interpretation of the spin transition in these systems as well as in other iron(II) complex compounds will be published in a separate report.[5]

2. Experimental Section

2.1. Preparations. (a) 2-Picolylamine. The ligand 2-picolylamine was synthesized following a prescription given by Craig and Hixon.[6] The boiling point (45–46 °C at 5 mmHg) and the IR spectrum of the product were found to agree well with literature data.

(b) $[Fe_{0.15}Zn_{0.85}(2\text{-pic})_3]Cl_2 \cdot C_2H_5OH$. The polycrystalline substance was prepared according to Sorai et al.[3b] in a glovebox under nitrogen atmosphere. $FeCl_2 \cdot 2H_2O$ (0.333 g, 2.04×10^{-3} mol) and $ZnCl_2$ (1.562 g, 1.161×10^{-2} mol) were dissolved in 25 mL of specially dried ethanol. After filtration a solution of 4.5 g (4.2×10^{-2} mol) of 2-picolylamine dissolved in 10 mL of ethanol was added. A yellow polycrystalline precipitated, which, after stirring for 12 h, was filtered off, washed several times with dry ethanol, and dried in vacuo. The yield was quantitative. Anal. Calcd for $Fe_{0.15}Zn_{0.85}(C_{20}H_{30}N_6OCl_2)$: C, 47.54; H, 5.94; N, 16.64; Fe, 1.663. Found: C, 47,42; H, 6.0; N, 17.23; Fe, 1.613.

The iron content was determined as follows. The sample was dissolved in a 1:1 mixture of fuming sulfuric acid and fuming nitric acid. After heating to dryness the residue was dissolved in dilute

0020-1669/78/1317-2509$01.00/0

hydrochloric acid. The photometric determination of the iron, in the presence of zinc, using 1,10-phenanthroline as complexing agent was performed according to the literature.[7] The analysis procedure was tested several times using mixed crystals of the title system with known content of iron and zinc. The relative error for the system with $x = 0.15$ was 0.8%; that for the system with $x = 0.0009$ was 5%.

(c) $[Fe_xZn_{1-x}(2\text{-pic})_3]Cl_2{\cdot}C_2H_5OH$ ($x = 0.029, 0.0009$). Because of the very low iron concentrations these samples had to be prepared with ^{57}Fe-enriched iron to obtain useful Mössbauer spectra. A total of 1.5 mg of enriched iron foil (81% ^{57}Fe, Rohstoff Einfuhr GmbH, Düsseldorf) was dissolved in concentrated hydrochloric acid under nitrogen atmosphere and heated to dryness. The procedure was repeated after adding hydrochloric acid and a very small quantity of natural iron to reduce a small fraction of ferric iron. A white powder of ^{57}Fe-enriched $FeCl_2{\cdot}2H_2O$ was obtained. All other operations to synthesize the mixed crystals are analogous to those described under (b).

Anal. Calcd for $Fe_xZn_{1-x}(C_{20}H_{30}N_6OCl_2)$, $x = 0.029$: C, 47.40; H, 5.92; N, 16.59. Found: C, 47.15; H, 6.02; N, 16.45; Fe, 0.31 (referred to total substance). Calcd for $x = 0.0009$: C, 47.30; H, 5.90; N, 16.54. Found: C, 46.85; H, 5.91; N, 16.44; Fe, 0.01.

For further purity control all samples were checked by IR spectroscopy in the range 500–4000 cm^{-1} using both Nujol mulls and poly(trifluorochloroethylene) mulls. All the IR spectra of the mixed crystals were practically identical revealing only characteristic bands of the ligand, which were, as a typical phenomenon of complex formation, slightly shifted to lower wavenumbers with respect to the free ligand. There was good agreement with literature data.[8-10] The OH band at 3344 cm^{-1} is indicative of the presence of ethanol solvent molecules in the crystal.

2.2. Mössbauer Measurements. Approximately 150 mg each of the three samples ($x = 0.15, 0.029, 0.0009$) was packed into Plexiglas absorber holders under a nitrogen atmosphere (glovebox) corresponding to ca. 0.057 mg cm^{-2} of ^{57}Fe in the case of $x = 0.15$ and ca. 0.014 mg cm^{-2} of ^{57}Fe in the case of $x = 0.0009$.

The Mössbauer spectra were recorded in transmission geometry using a ^{57}Co/Rh source (17 mCi, Radiochemical Centre, Amersham, England) kept at room temperature and moved relative to the absorber with a conventional triangular wave form vibrator of the Kankeleit type.[11] The spectrometer was operated in the multiscaling mode using a 400 channel analyzer (SA 41, Intertechnique). The relative velocity scale was calibrated on the basis of the hyperfine spectrum of metallic iron. A proportional counter (Reuter-Stokes, 93% Xe/7% CH_4) was used to detect the 14.4-keV γ radiation. The absorber temperatures were varied between 5 and 300 K employing a MD4A type cryostat of Oxford Instruments/England and controlled with a Mark 2 controller from Oxford Instruments. For the temperature measurements we used a calibrated Si diode (DT 100 P).

A sum of Lorentzian lines was fitted to the measured spectra using a least-squares iteration computer program.

3. Results and Discussion

A selection of representative Mössbauer spectra of $[Fe_{0.029}Zn_{0.971}(2\text{-pic})_3]Cl_2{\cdot}C_2H_5OH$ at 200, 130, 90, 70, 40, and 5 K are shown in Figure 1. Zero velocity corresponds to the isomer shift of metallic iron vs. a ^{57}Co/Rh source at 298 K. At high temperatures ($T \geq 200$ K) the Mössbauer spectra showed in all cases only one quadrupole doublet with a quadrupole splitting of $\Delta E_Q \approx 2.1$ mm s^{-1} and an isomer shift of $\delta \approx 1$ mm s^{-1}; these values and also the pronounced temperature dependence of the quadrupole splitting are characteristic of iron(II) in the high-spin (HS) state, $^5T_2$ (O_h). Below ca. 200 K the relative intensity of this doublet decreases gradually with decreasing temperature, and a new quadrupole doublet with $\Delta E_Q \approx 0.4$ mm s^{-1} and $\delta \approx 0.55$ mm s^{-1}, which is typical for iron(II) in the low-spin state, $^1A_1$ (O_h), appears with growing relative intensity. At temperatures ≤40 K only the low-spin quadrupole doublet is left in the spectra.

The data of the isomer shift δ (with respect to metallic iron), quadrupole splitting ΔE_Q, and area fraction F derived from the least-squares fitted spectra for both the high-spin (HS) and the low-spin (LS) doublets of iron(II) as a function of temperature are given for the three systems under study ($x = 0.15, 0.029, 0.0009$) in Table I. The data of the experimental line width Γ has not been listed here; its average value is 0.27 ± 0.03 mm s^{-1} for both the high-spin (HS) and the low-spin (LS) doublet.

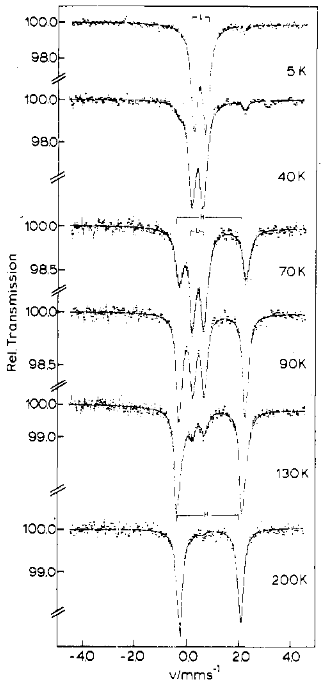

Figure 1. ^{57}Fe Mössbauer spectra of $[Fe_{0.029}Zn_{0.971}(2\text{-pic})_3]Cl_2{\cdot}C_2H_5OH$ at various temperatures taken with a ^{57}Co/Rh source at 293 K. Zero velocity refers to the isomer shift of metallic iron. H is the high-spin doublet and L is the low-spin doublet of iron(II).

At a given temperature the isomer shift, the quadrupole splitting, and the resonance line width of both the high-spin and the low-spin doublets of iron(II) are independent of the dilution degree x within the experimental errors. This has also been observed in the mixed-crystal systems with x ranging from 0.2 to 1.0[3a] and supports the assumption of random mixing of iron and zinc to form ideal solid solutions with no noticeable influence of the metal substitution on the valence electronic structure of iron. The broadening of the resonance lines varies between 20 and 60%, as compared to twice the natural line width of $2\Gamma_{nat} = 0.19$ mm s^{-1}, and most probably stems from the usual sources of finite absorber thickness and slight inhomogeneities of the hyperfine interactions.

The isomer shift of the high-spin doublet (HS) changes somewhat with temperature mostly due to the second-order Doppler (SOD) shift. The temperature effect is less pronounced on the isomer shift of the LS doublet.

There is essentially no temperature influence on the quadrupole splitting of the LS doublet, whereas the ΔE_Q values of the HS doublet change markedly with varying temperature. As has been suggested by Ingalls[13] and demonstrated successfully later on by various authors[14-18] it is possible to extract information about the nature of the electronic state of a high-spin iron(II) species from the temperature dependence of the quadrupole splitting. This can be calculated considering a Boltzmann distribution of valence electrons over all thermally accessible levels resulting from low-symmetry crystal field distortions (in the present case trigonal and/or rhombic distortions) and spin–orbit coupling.

With the aid of a computer program written by K. M. Hasselbach in our laboratory,[19] we have calculated the energy level splitting of the $^5T_{2g}$ (O_h) state due to trigonal and rhombic field distortions, respectively, and spin–orbit coupling. The results are depicted in Figure 2 for the two most probable local symmetries around the iron atom, viz., C_{3v} (facial isomer) in Figure 2a, and C_{2v} (peripheral isomer) in Figure 2b. We have

Table I. Isomer Shift δ (Relative to Metallic Iron at 293 K), Quadrupole Splitting ΔE_Q, and Fractional Area F for the High-Spin Doublet (HS) and the Low-Spin Doublet (LS) as a Function of Temperature in $[Fe_xZn_{1-x}(2\text{-pic})_3]Cl_2\cdot C_2H_5OH$ with (a) $x = 0.15$, (b) $x = 0.029$, and (c) $x = 0.0009$

	δ^{Fe}/mm s^{-1} [a]		ΔE_Q/mm s^{-1}		F/%[b]	
T/K	HS	LS	HS	LS	HS	LS
(a) $x = 0.15$						
5.5		0.555 (3)		0.444 (2)		>99
40	1.11 (6)	0.545 (3)	2.49 (6)	0.431 (2)	8 (7)	92 (5)
65	1.07 (2)	0.549 (3)	2.58 (2)	0.431 (2)	22 (5)	78 (3)
77[d]	1.062 (9)	0.539 (8)	2.55 (2)	0.428 (3)	39 (5)	61 (5)
85[d]	1.06 (1)	0.539 (9)	2.56 (3)	0.433 (8)	45 (6)	55 (5)
90[d]	1.065 (9)	0.539 (8)	2.53 (2)	0.428 (8)	52 (6)	48 (6)
110[d]	1.045 (9)	0.53 (2)	2.48 (2)	0.42 (2)	66 (9)	34 (8)
130	1.072 (7)	0.52 (3)	2.53 (2)	0.41 (3)	84 (7)	16 (6)
150[d]	1.036 (7)	0.54 (5)	2.48 (2)	0.42 (4)	85 (6)	15 (7)
180	1.038 (7)	0.54 (7)	2.43 (2)	0.33 (8)	93 (8)	7 (7)
200	1.033 (7)		2.38 (2)		>98	
220	1.021 (8)		2.31 (2)		~100	
260	0.991 (8)		2.18 (2)		~100	
300	0.957 (9)		2.06 (2)		~100	
(b) $x = 0.029$						
5	1.11[c]	0.556 (2)	2.46[c]	0.444 (2)	<2	>98
16	1.11 (4)	0.557 (2)	2.47 (6)	0.452 (2)	<4	>95
26	1.11[c]	0.554 (3)	2.47[c]	0.438 (3)	<3	>97
40	1.10 (4)	0.548 (4)	2.54 (7)	0.438 (3)	6 (4)	94 (5)
65	1.07 (1)	0.543 (3)	2.58 (2)	0.433 (3)	28 (4)	72 (4)
70	1.07 (1)	0.541 (6)	2.58 (2)	0.437 (4)	39 (5)	61 (5)
78.8	1.073 (8)	0.537 (6)	2.57 (2)	0.432 (4)	48 (4)	52 (4)
85	1.065 (8)	0.542 (8)	2.56 (2)	0.434 (6)	55 (4)	45 (4)
90	1.067 (7)	0.534 (8)	2.56 (2)	0.441 (7)	58 (5)	42 (5)
110	1.058 (7)	0.53 (3)	2.54 (2)	0.43 (3)	73 (4)	27 (4)
130	1.052 (7)	0.55 (3)	2.50 (2)	0.46 (3)	83 (5)	17 (5)
150	1.047 (7)	0.49 (4)	2.48 (2)	0.42 (4)	89 (5)	11 (5)
180	1.034 (7)	0.51[c]	2.40 (2)	0.42[c]	>95	<5
200	1.024 (7)	0.51[c]	2.35 (2)	0.42[c]	>97	<4
220	1.015 (7)		2.31 (2)		~100	
260	0.986 (7)		2.18 (2)		~100	
300	0.957 (7)		2.04 (2)		~100	
(c) $x = 0.0009$						
5.5		0.55 (3)		0.43 (1)		>99
20		0.544 (9)		0.432 (7)		>99
40	1.10[c]	0.543 (10)	2.54[c]	0.418 (8)	<6	>94
60	1.09 (2)	0.548 (8)	2.55 (3)	0.424 (7)	29 (9)	71 (8)
81	1.045 (6)	0.547 (8)	2.50 (1)	0.425 (7)	53 (5)	47 (4)
85.5	1.081 (8)	0.560 (9)	2.60 (2)	0.450 (8)	58 (7)	42 (6)
90	1.047 (7)	0.541 (9)	2.52 (1)	0.431 (9)	65 (6)	35 (6)
110	1.044 (7)	0.52 (2)	2.49 (1)	0.43 (2)	74 (6)	26 (7)
130	1.061 (7)	0.54 (5)	2.54 (1)	0.41 (4)	84 (6)	16 (8)
150	1.058 (7)	0.51 (4)	2.50 (1)	0.40 (4)	89 (9)	11 (6)
180	1.016 (7)	0.54[c]	2.36 (1)	0.42[c]	95 (9)	5 (4)
200	0.986 (9)	0.54[c]	2.30 (2)	0.42[c]	93 (9)	<7
300	0.95 (1)	0.54[c]	2.06 (3)	0.42[c]	>94	<7

[a] Read 1.11 (6) = 1.11 + 0.06. [b] Read 92.5 (46) = 92.5 ± 4.6. [c] Parameter not varied. [d] ^{57}Co/Cu as source; ^{57}Co/Rh in all other cases.

considered only the perturbation on the $^5T_{2g}$ (O_h) state and not on the ^5E_g (O_h), because—as we have proven in separate calculations of the electric field gradient (EFG) as a function of temperature including all sublevels resulting from crystal field and spin–orbit perturbation on $^5T_{2g}$ (O_h) and ^5E_g (O_h)—the multiplet of the ^5E_g (O_h) state being higher in energy than that of the $^5T_{2g}$ (O_h) state by about 12 500 cm^{-1} is not thermally accessible to any appreciable extent and therefore does not contribute to the EFG. We have taken the effective perturbation operator to be

$$\hat{H}' = \hat{V}_a + \hat{V}_r + \alpha_\lambda^2\lambda_0\hat{L}\cdot\hat{S} \tag{1}$$

with

$$\hat{V}_a = -\tfrac{1}{3}\epsilon_a(\hat{L}_z^2 - 2)$$

$$\hat{V}_r = \frac{\epsilon_r}{2}(\hat{L}_+^2 + \hat{L}_-^2)$$

$\hat{V}_a$ refers to the axial distortion, trigonal in the C_{3v} case and tetragonal in the C_{2v} case, resulting in the splitting parameter ϵ_a. $\hat{V}_r$ refers to the additional rhombic distortion in the C_{2v} case resulting in the parameter ϵ_r. After diagonalization of the perturbation matrix we have used the symmetry-adapted wave functions and adjusted the general expression for the temperature dependence of the quadrupole splitting[13]

$$\Delta E_Q(T) = \frac{1}{2}e^2Q(1-R)\langle r^{-3}\rangle_{3d}{}^0\,\alpha_c^2[F(\epsilon_{a(r)},\alpha_\lambda^2\lambda_0,T)] \times \left(1 + \frac{\eta^2(T)}{3}\right)^{1/2} + \Delta E_Q{}^c \tag{2}$$

to the experimental values of ΔE_Q. The quantities of eq 2 have the usual meaning as described, e.g., in ref 16 and 17. The "best-fit values" for the parameters ϵ_a, ϵ_r, α_c^2, and α_λ^2 (covalency factors taking care of the reduction of the free ion radial expansion $<r^{-3}>_{3d}{}^0$ and the free ion spin–orbit coupling constant λ_0 upon complex formation), and $\Delta E_Q{}^c$ (temperature-independent contribution to the quadrupole splitting ΔE_Q) are listed in Table II as a function of the dilution degree x.

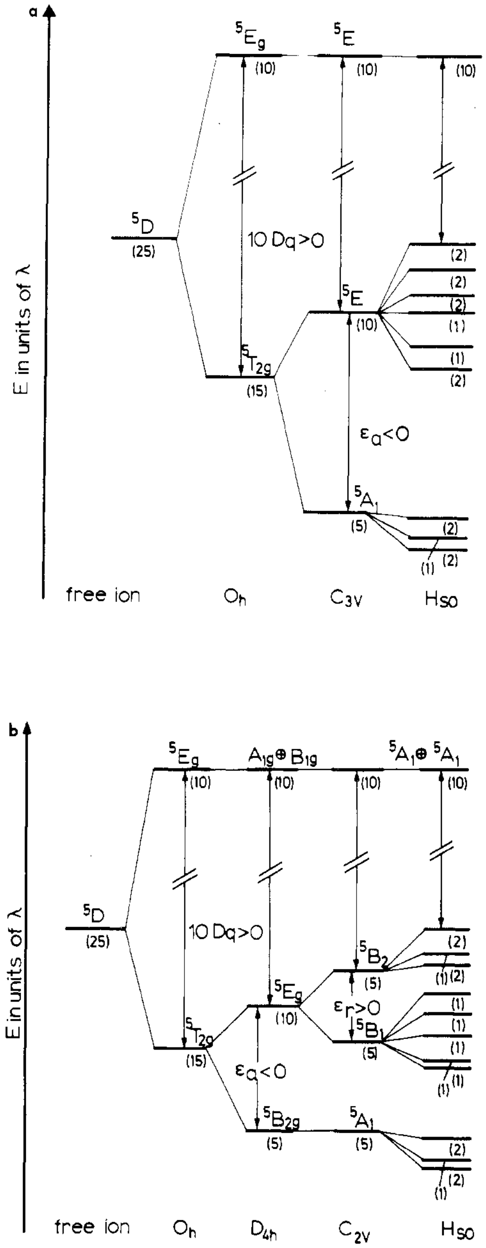

Figure 2. Energy-level diagrams considering the effect of (a) axial (trigonal in case of C_{3v} symmetry, parameter ϵ_a) and (b) axial and rhombic (tetragonal and digonal in case of C_{2v} symmetry, parameters ϵ_a and ϵ_r) crystal field distortions and spin–orbit coupling, derived from the temperature dependence of the ^{57}Fe quadrupole splitting in $[Fe_xZn_{1-x}(2\text{-pic})_3]Cl_2{\cdot}C_2H_5OH$. Spacings in units of the spin–orbit coupling parameter are (a) $\lambda(C_{3v})$ = 82.4 cm^{-1} and (b) $\lambda(C_{2v})$ = 87.4 cm^{-1}.

Table II. Electronic Parameters of the High-Spin Iron(II) Species in $[Fe_xZn_{1-x}(2\text{-pic})_3]Cl_2{\cdot}C_2H_5OH$ ($0.0009 \leqslant x \leqslant 1.0$) Derived from the Temperature Dependence of the Quadrupole Doublet with the Assumption of (a) C_{3v} and (b) C_{2v} Local Symmetry

x^a	ϵ_a/cm^{-1} [b]	ϵ_r/cm^{-1} [c]	α_c^2 [d]	α_λ^2 [d]	ΔE_Q[c]/mm s^{-1} [c]	sign V_{zz}
			(a) C_{3v} Symmetry			
0.0009	−457		0.79	0.79	0.34_2	−
0.029	−498		0.73	0.67	0.32_5	−
0.15	−509		0.76	0.69	0.44_8	−
0.2	−426		0.77	0.91	0.34_7	−
0.6	−433		0.77	0.88	0.34_5	−
0.8	−442		0.76	0.89	0.32_8	−
1.0	−441		0.77	0.96	0.34_7	−
			(b) C_{2v} Symmetry			
0.0009	−378	248	0.82	0.87	0.07_8	+
0.029	−363	225	0.72	0.85	0.38_8	+
0.15	−403	312	0.74	0.79	0.12_4	+
0.2	−380	206	0.74	0.87	-0.00_4	+
0.6	−400	238	0.74	0.88	-0.03_0	+
0.8	−400	222	0.74	0.88	-0.03_6	+
1.0	−386	222	0.75	0.94	0.02_1	+

[a] Calculations for x = 0.2, 0.6, 0.8, 1.0 performed by M. Sorai in our laboratory in connection with Mössbauer-effect studies in these systems.[3a] [b] Average error 10%. [c] Average error 10%. [d] Average error 15%.

Table III. Transition Temperature T_C as a Function of Dilution Degree x in $[Fe_xZn_{1-x}(2\text{-pic})_3]Cl_2{\cdot}C_2H_5OH$, Derived from $\gamma_{HS}(T)$ Curves for Variable x

x	T_C/K^a from $\gamma_{HS}(T)$	Ref
1.0	122	3a
0.8	115	3a
0.6	107	3a
0.2	90	3a
0.15	88	this work
0.029	80	this work
0.0009	77	this work

[a] Average error ±2.5 K.

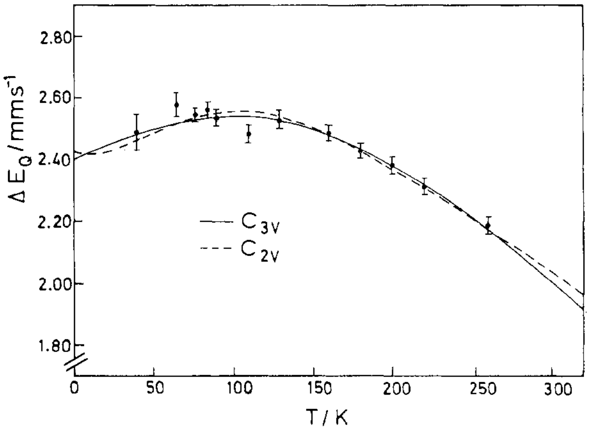

Figure 3. Temperature dependence of the quadrupole splitting ΔE_Q of the high-spin iron(II) species in $[Fe_{0.15}Zn_{0.85}(2\text{-pic})_3]Cl_2{\cdot}C_2H_5OH$. The solid and the dashed curves have been calculated assuming C_{3v} and C_{2v} symmetries, respectively, with the parameter values given in Table II under x = 0.15.

Figure 3 shows, as an example, the calculated curves (solid line for C_{3v}, dashed line for C_{2v} symmetry) and the experimental values of the quadrupole splitting of the HS state of iron(II) in $[Fe_{0.15}Zn_{0.85}(2\text{-pic})_3]Cl_2{\cdot}C_2H_5OH$ as a function of temperature. Similar pictures with satisfactory agreement between theory and experiment were obtained for the other systems with various x. The most essential findings from this examination are the following.

(i) The sign of ϵ_a turned out to be negative in all cases. This implies that the ^5A (C_{3v}) or $^5A_2$ (C_{2v}) terms are the lowest states in the HS configuration.

(ii) The temperature dependence of the quadrupole splitting apparently does not permit a conclusive statement as to which of the two considered local symmetries, C_{3v} or C_{2v}, is the most probable one in the systems under study. The $\Delta E_Q(T)$ functions calculated for the two symmetry cases match equally well the measured data. Further information could be received from Mössbauer effect experiments in external magnetic fields which, in general, enable one to distinguish between the sign of the EFG (V_{zz}). Such experiments are presently underway using a cryomagnetic system.

(iii) There are no definite trends in the values of any of the electronic parameters as a function of x. In all cases there is random distribution about a certain average value. This

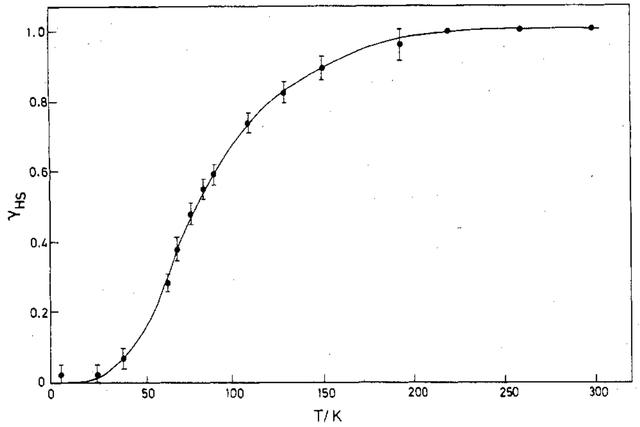

Figure 4. Temperature dependence of the area fraction γ_{HS} of the high-spin iron(II) resonance lines of $[\mathrm{Fe}_{0.029}\mathrm{Zn}_{0.971}(2\text{-pic})_3]\mathrm{Cl}_2\cdot\mathrm{C}_2\mathrm{H}_5\mathrm{OH}$.

indicates that the electronic structure of the high-spin iron(II) species is practically independent of the dilution degree x.

The gradual spin transition between the high-spin and low-spin states as a function of temperature may be followed quantitatively by extracting the area fraction γ_{HS} of the HS resonance lines from the variable-temperature Mössbauer spectra, as we have described in a previous report.[3a] We are aware of the fact that this procedure incorporates a systematic error, because the Debye–Waller factor for the HS state (f_{HS}) generally is different from that of the LS state (f_{LS}) ($f_{HS} < f_{LS}$[17,20]), and therefore the relative amounts of the high-spin and low-spin species of iron(II) are not equal to the relative area fractions of the corresponding resonance lines. In principle, it is possible to evaluate the Debye–Waller factors f_{HS} and f_{LS} with additional aid of another method, e.g., variable-temperature susceptibility or far-infrared measurements, and to determine the relative amounts of the iron(II) species with different spin state. This way, however, is very tedious, and it does not promise any significant improvement of the results of our further thermodynamic treatment of the high-spin $\rightleftharpoons$ low-spin transition. For example, we have estimated that, taking the ratio f_{LS}/f_{HS} to ~1.2 as has been found for an iron(II) complex compound with temperature-induced magnetic crossover,[20] the area fraction γ_{HS} of the high-spin resonance lines comes out too small by

$$\Delta\gamma_{HS} = -\gamma_{HS}\left(\frac{1}{\gamma_{HS} + \gamma_{LS}(f_{LS}/f_{HS})} - 1\right) \approx 0.045$$

in the worst case; i.e., the relative amount of the high-spin iron(II) species is ≤4.5% larger than the much more easily attainable area fraction γ_{HS}. This leads to a systematic increase of the observed transition temperature by 2–3 K. Plotting the area fraction γ_{HS} as a function of temperature yields diagrams as exemplified in Figure 4 for the system $[\mathrm{Fe}_{0.029}\mathrm{Zn}_{0.971}(2\text{-pic})_3]\mathrm{Cl}_2\cdot\mathrm{C}_2\mathrm{H}_5\mathrm{OH}$. The transition curves $\gamma_{HS}(T)$ for the very dilute systems ($x = 0.15, 0.029, 0.0009$) of the present study complement nicely those obtained in earlier studies[3a] in the sense that, with decreasing iron concentration, the maximum slope of the transition curve $\gamma_{HS}(T)$ is shifted to lower temperature, the transition temperature T_C ($\gamma_{HS} = \gamma_{LS} = 0.5$) decreases, and the slope of the transition curve near T_C becomes less steep. $T_C(x)$ data derived from $\gamma_{HS}(T)$ curves for the whole range of x studied so far ($0.0009 \le x \le 1.0$) are plotted in Figure 5.

These experimental findings support the model of cooperative spin transition suggested by Sorai and Seki[2] and already extensively discussed in a previous report.[3a] The essential features of this model are the following. The driving force of the spin transition is the entropy difference between the high-spin state ($S = 2$) and the low-spin state ($S = 0$); the magnetic part, $R \ln (2S + 1)$, as well as the vibrational contribution to the total entropy, is larger in the high-spin state than in the low-spin state. The spin transition in a primary iron center is spontaneously followed by a modulation of the normal modes of vibration, particularly of the iron–ligand stretching vibrations and the ligand–iron–ligand deformation vibrations which have been found by far-infrared spectroscopy in other magnetic crossover systems of iron(II)[17,21] to exhibit differences of about 250 wavenumbers between the stretching vibrations of the HS and the LS state and about 150 wavenumbers between the deformation vibrations of the HS and the LS state, with the LS state having the stronger force constants in each case. The modulation of the vibrational structure around the primary spin transition center will be "communicated" to neighboring complex molecules, most probably via hydrogen bonding chains as has been supported recently by experiments with deuterated systems.[22] Secondary spin transitions in neighboring $[\mathrm{Fe}\overset{\frown}{\mathrm{NN}}'_3]$ clusters will take place immediately after the incoming "communication" has reached the first coordination sphere of such $[\mathrm{Fe}\overset{\frown}{\mathrm{NN}}'_3]$ clusters and modulated the normal modes of vibrations to a sufficient extent. According to this model secondary spin transitions will take place in $(n - 1)$ $[\mathrm{Fe}\overset{\frown}{\mathrm{NN}}'_3]$ clusters, which form a so-called "cooperative region" around the primary spin change center.

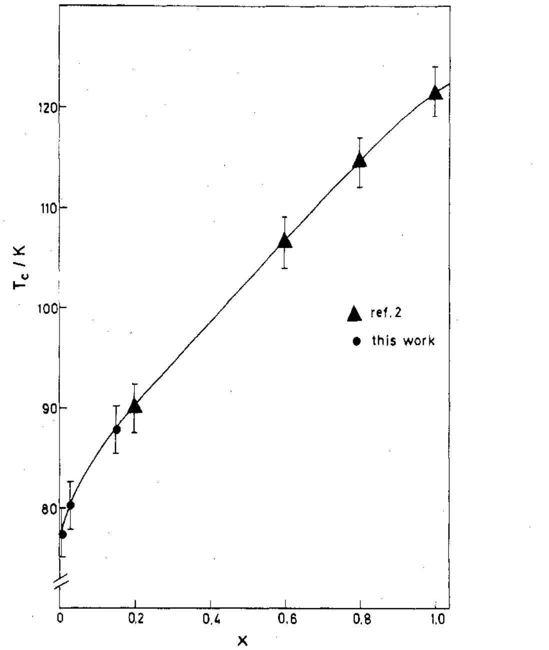

Figure 5. Concentration dependence of the spin transition temperature T_C for $[\mathrm{Fe}_x\mathrm{Zn}_{1-x}(2\text{-pic})_3]\mathrm{Cl}_2\cdot\mathrm{C}_2\mathrm{H}_5\mathrm{OH}$.

The steepness of the transition curve $\gamma_{HS}(T)$ appears to be a measure for the strength of the coupling between the change in electronic structure of the primary iron center and the intra- and intermolecular vibrations. Strong coupling in this sense is expected to give rise to a steep (abrupt) transition curve $\gamma_{HS}(T)$, similar to that in $[\mathrm{Fe(phen)}_2(\mathrm{NCS})_2]$ for instance,[23] and relatively large cooperative regions in terms of the number n, which has been estimated to be 80–100 for $[\mathrm{Fe(phen)}_2(\mathrm{NCS})_2]$.[2] Weak coupling should result in gradual spin changes, similar to the present systems; accordingly the number n should be much smaller. On these grounds the decreasing steepness of the $\gamma_{HS}(T)$ curves of the present and of the earlier studies[3a] as a function of x seems to be indicative of a weakening of the coupling strength going along with a decrease of n.

In a separate publication[5] it will be shown in the framework of a phenomenological and statistical thermodynamic treatment of the spin transition that the domain size (number n) strongly depends on x; the calculations for the weakly coupling title system have yielded $n \approx 4$ for $x = 1$ and $n \approx 1$ for $x = 0.0009$. There we shall also treat quantitatively the pronounced concentration dependence of the transition temperature T_C as evidenced in Figure 5. Here we shall restrict ourselves to the following qualitative explanation.

The spin transition is expected to be accompanied by an enthalpy change $\Delta H°$ which may be considered to be composed of two parts:

$$\Delta H° = \Delta H°_{Fe} + \Delta H°_{coop} \qquad (3)$$

$\Delta H°_{Fe}$ describes the enthalpy change of 1 mol of individual complex iron molecules (comprises contributions from the changes in electronic structure, in intramolecular vibrations, and in intramolecular electron–phonon interaction). $\Delta H°_{coop}$ describes the enthalpy change due to a change of the intermolecular interactions between the iron atoms of like spin in a cooperative domain as a result of a spin transition. $\Delta H°_{coop}$ can stabilize a domain as a unit with a particular spin state. The falling tendency of T_C with decreasing iron concentration can be rationalized in terms of a stronger stabilization of the low-spin state over the high-spin state by cooperative interaction, $\Delta H°_{coop} = H°_{coop}(LS) - H°_{coop}(HS) > 0$. Under the condition of $kT \geq \Delta H°_{coop}$, the influence of this stabilization effect is reduced and the spin transition takes place. If the iron concentration is lowered, the cooperative interaction becomes less effective and therefore $\Delta H°_{coop}$ decreases. This in turn means that the condition $kT \geq \Delta H°_{coop}$ will be fulfilled at a lower temperature; i.e., spin transition will take place at a somewhat lower temperature and T_C will decrease.

The concentration dependence of T_C as depicted in Figure 5 follows practically a linear function from $x = 1.0$ down to $x \approx 0.15$. At $x \lesssim 0.15$, $T_C(x)$ decreases more rapidly and thus deviates from the extrapolated straight line implying that the high-spin state is favored more effectively than in the x range above. In more and more cases the "communication" of a primary spin transition travels now through a $[Zn\widehat{NN'}_3]$ cluster in the beginning. As there is no spin change possible in the zinc complex molecule, one would not expect any significant modulation of its normal vibrations and therefore the cooperative effect should be reduced as compared to a $[Fe\widehat{NN'}_3]$ molecule.

As the transition temperature T_C appears to bear particular importance in the framework of the domain model by Sorai and Seki, other ways of determining T_C, e.g., by heat capacity measurements, would be highly desirable. Such data are not yet available, and the use of a formal T_C to denote the temperature at which equal amounts of high-spin and low-spin molecules are present is a tentative one.[24]

Acknowledgment. The authors wish to thank the Deutsche Forschungsgemeinschaft, the Bundesministerium für Forschung und Technologie, and the Fonds der Chemischen Industrie for financial support. The help of Miss E. Börner concerning the metal analysis is gratefully acknowledged. For stimulating discussions and assistance in carrying out experiments we thank R. Grimm, Dr. K. M. Hasselbach, H. Köppen, and W. Müller.

Registry No. $[Fe(2\text{-pic})_3]Cl_2$, 18433-69-7; $[Zn(2\text{-pic})_3]Cl_2$, 61919-63-9.

References and Notes

(1) Work performed in partial fulfillment of the Diplomarbeit by H. G. Steinhäuser; first presented at the International Conference on Mössbauer Spectroscopy, 1977, Bucharest, Romania.

(2) M. Sorai and S. Seki, *J. Phys. Soc. Jpn.*, **33**, 575 (1972); *J. Phys. Chem. Solids*, **35**, 555 (1974).

(3) (a) M. Sorai, J. Ensling, and P. Gütlich, *Chem. Phys.*, **18**, 199 (1976); (b) M. Sorai, J. Ensling, K. M. Hasselbach, and P. Gütlich, *ibid.*, **20**, 197 (1977).

(4) G. A. Renovitch and W. A. Baker, Jr., *J. Am. Chem. Soc.*, **89**, 6377 (1967).

(5) H. Köppen, R. Link, H. G. Steinhäuser, and P. Gütlich, *J. Chem. Phys.*, in press.

(6) L. C. Craig and R. M. Hixon, *J. Am. Chem. Soc.*, **53**, 4368 (1931).

(7) H. Ginsberg, "Leichtmetallanalyse", W. de Gruyter & Co., West Berlin, 1965, p 200.

(8) D. H. Williams and J. Fleming, "Spektroskopische Methoden in der organischen Chemie", Georg Thieme Verlag, Stuttgart, 1971.

(9) K. Nakamoto, "Infrared Spectra of Inorganic and Coordination Compounds", Wiley, New York, N.Y., 1963.

(10) L. J. Bellamy, "Ultrarot-Spektren und chemische Konstitution", Steinkopf-Verlag, Darmstadt, 1966.

(11) E. Kankeleit, *Rev. Sci. Instrum.*, **35**, 194 (1964).

(12) H. G. Steinhäuser, Diplomarbeit, 1977, Chemistry Department, University of Mainz.

(13) R. Ingalls, *Phys. Rev.*, **133**, 787 (1964).

(14) T. C. Gibb, *J. Chem. Soc. A*, 1439 (1968).

(15) J. Fleisch, P. Gütlich, and K. M. Hasselbach, *Inorg. Chim. Acta*, **17**, 51 (1976).

(16) J. Fleisch, P. Gütlich, K. M. Hasselbach, and W. Müller, *Inorg. Chem.*, **15**, 958 (1976).

(17) J. Fleisch, P. Gütlich, and K. M. Hasselbach, *Inorg. Chem.*, **16**, 1979 (1977).

(18) W. Neuwirth and H. J. Schröder, *Z. Phys. B*, **23**, 71 (1976).

(19) K. M. Hasselbach, Laborbericht /77, Institut für Anorganische Chemie und Analytische Chemie, University of Mainz.

(20) E. König and G. Ritter, "Mössbauer Effect Methodology", Vol. 9, Plenum Press, New York, N.Y., 1974, p 3.

(21) J. H. Takemoto and B. Hutchinson, *Inorg. Nucl. Chem. Lett.*, **8**, 769 (1972); *Inorg. Chem.*, **12**, 705 (1973).

(22) P. Gütlich, R. Link, H. G. Steinhäuser, and G. Sudheimer, to be published.

(23) W. A. Baker, Jr., and H. M. Bobonich, *Inorg. Chem.*, **3**, 1184 (1964).

(24) After submission of this paper, a crystal structure study on $[Fe(2\text{-pic})_3]Cl_2 \cdot EtOH$ by a Japanese group came to our attention showing that the $[Fe(2\text{-pic})_3]^{2+}$ complex ion has peripheral rather than facial geometry: M. Mikami, M. Konno, and Y. Saito, Abstracts, Annual Meeting of the Chemical Society of Japan, Tokyo, 1978, No. 2J32.